OPEN ACCESS

University of BRISTOL

Peer reviewed version

License (if available):
Unspecified

Link to published version (if available):
10.1126/science.aah5982

Link to publication record in Explore Bristol Research
PDF-document

University of Bristol - Explore Bristol Research
General rights

Ultrastructural Evidence for Synaptic Scaling Across the Wake/sleep Cycle

Luisa de Vivo[1], Michele Bellesi[1,3], William Marshall[1], Eric A Bushong[2], Mark H Ellisman[2,4],

Giulio Tononi[1*] and Chiara Cirelli[1*]

[1] Department of Psychiatry, University of Wisconsin-Madison, 6001 Research Park Blvd, Madison, WI 53719 USA
[2] National Center for Microscopy and Imaging Research, University of California San Diego, 9500 Gilman Drive, La Jolla, CA 92093 USA
[3] Department of Experimental and Clinical Medicine, Section of Neuroscience and Cell Biology, Università Politecnica delle Marche, Ancona, Italy
[4] Department of Neurosciences, University of California San Diego, School of Medicine, 9500 Gilman Drive, La Jolla, CA 92093 USA

* Corresponding author. E-mail: ccirelli@wisc.edu; gtononi@wisc.edu.

It is assumed that synaptic strengthening and weakening balance throughout learning to avoid runaway potentiation and memory interference. However, energetic and informational considerations suggest that potentiation should occur primarily during wake, when animals learn, and depression during sleep. We measured 6,920 synapses in mouse motor and sensory cortices using 3D-electron microscopy. The axon-spine interface (ASI) decreased ~18% after sleep compared to wake. This decrease was proportional to ASI size, indicative of scaling. Scaling was selective, sparing synapses that were large and lacked recycling endosomes. Similar scaling occurred for spine head volume, suggesting a distinction between weaker, more plastic synapses (~80%) and stronger, more stable synapses. These results support the hypothesis that a core function of sleep is to renormalize overall synaptic strength increased by wake.

The cerebral cortex contains 16 billion neurons in humans, 14 million in mice(*1*), and each neuron harbors thousands of synapses(*2*). Of the billions of cortical synapses of adult mice, ~80% are excitatory and the majority of these are on dendritic spines(*3*). Spine size is tightly correlated with synaptic strength(*3, 4*): the area of the postsynaptic density (PSD), the area of the axon-spine interface (ASI), and the volume of the spine head (HV) are strongly correlated among themselves and with the number of vesicles in the presynapse(*5-8*), the number of synaptic AMPA receptors (AMPAR(*9*)), and the amplitude of AMPAR-mediated synaptic currents(*10, 11*).

Changes in synaptic strength are the primary mechanisms mediating learning and memory(*12, 13*). Synaptic potentiation and depression must be balanced to avoid either saturation or obliteration of neural signaling and memory traces(*14*), and it is usually assumed that overall synaptic strength is regulated throughout learning(*15*). The synaptic homeostasis hypothesis (SHY)(*16*) argues, however, that owing to energy and signaling requirements, learning should occur primarily through synaptic potentiation during wake, leading to a net increase in synaptic strength. This is because sparsely firing neurons can ensure that coincidences in their inputs learned during wake are signaled throughout the brain only if the connections relaying such coincidences are strengthened, not weakened. Overall synaptic renormalization by net weakening should occur during sleep, when animals are disconnected from the environment. The reason is that spontaneous neural activity can sample memories in a comprehensive and fair manner only if the brain is offline, without being at the mercy of current environmental inputs. Sleep can thus promote the acquisition, consolidation and integration of new information, as well as restore cellular function(*16, 17*).

Because stronger synapses are larger and weaker ones smaller(*3, 4*), SHY makes an intriguing prediction: billions of cortical excitatory synapses should increase in size after wake and decrease after sleep, independent of circadian time. Furthermore, while synaptic renormalization should affect a majority of synapses, it should also be selective, to allow for both stability and plasticity(*16-18*).

We used serial block-face scanning electron microscopy (SBEM)(*19*) to obtain direct, high-resolution 3D volume measurements of synaptic size during the wake/sleep cycle and across thousands of synapses in two regions of mouse cortex. Brains were collected from 3 groups of mice (4 mice/group; Fig.1A): S (sleep) mice spent at least 75% of the first ~7h of the light period asleep, EW (enforced wake) mice were kept awake during that time by exposure to novel objects, and SW (spontaneous wake) mice spent at least 70% of the first ~7h of the dark period spontaneously awake (Fig.1B). S mice were compared to both SW and EW mice, to tease apart sleep/wake effects from potential confounding factors due to time of day, light exposure, and stimulation/stress associated with enforced wake. In each mouse we sampled layer 2 of primary motor (M1) and primary somatosensory (S1) cortices. In these areas and

layers activity-dependent structural plasticity is well documented(*3*). Blocks of cortical tissue (~25x25x13-25µm) were acquired, automatically aligned, and spiny dendritic segments were randomly selected within each block, balanced in size across groups (diameter = 0.86 ± 0.05 µm, mean ± std; Table S1), and manually segmented by trained annotators blind to experimental condition (Fig.1C,D; Methods). Within each dendritic segment all protrusions (also called "spines"(*3*)) were annotated, including spines forming synapses and a minority that lacked synapses (~13% of all protrusions; Table S1). Across all mice, 168 dendritic segments were segmented (101 in M1; 67 in S1; Fig.1D, Fig.S1), for a total of 8,427 spines, of which 7,149 formed a synapse. Synapses were defined by the presence of a presynaptic bouton with at least 2 synaptic vesicles within a 50 nm distance from the cellular membrane facing the spine, a visible synaptic cleft, and a PSD. In spines forming a synapse, ASI, HV, as well as vesicles, tubules and multivesicular bodies (MVBs) that together form the non-smooth endoplasmic reticulum (non-SER) compartment(*20*), and the spine apparatus were segmented (Fig.1E,F) (see Methods). After excluding incomplete synapses, 6,920 spines with a synapse contributed to the final analysis (Tables S1, S2).

ASI and PSD are strongly correlated with each other and both become larger after synaptic potentiation(*6-8*). We focused on ASI - the surface of direct contact between axonal bouton and spine - as a structural measure of synaptic strength because in SBEM images its exact borders are easier to identify than those of the PSD(*21*). First, we asked whether ASI sizes change as a function of wake and sleep using a linear mixed effects model that included mouse and dendrite as random effects, condition (SW, EW, S) and brain region (S1, M1) as categorical fixed effects, and dendrite diameter as a linear fixed effect. Condition had a strong effect on ASI (χ^2 = 10.159, df = 2, p = 0.0062), which did not interact with either brain region or dendrite diameter. Post-hoc analysis (adjusted for multiple comparisons) found that ASI sizes after sleep were reduced on average by 18.9% relative to spontaneous wake (p = 0.001), and by 17.5% compared to enforced wake (p = 0.003; Fig.2A; see Methods, LME Model for ASI). Spontaneous and enforced wake did not differ (SW vs. EW, -1.7%; p = 0.957). Thus, ASI sizes decrease with sleep on average by ~18% relative to both spontaneous and enforced wake, independent of time of day. There was instead no difference across groups in the distribution of dendrite (p = 0.248) and mitochondrial (p = 0.445) diameters, ruling out overall tissue shrinkage after sleep (Fig. S2).

Consistent with the range of PSD and spine sizes in mouse somatosensory and auditory cortex(*22, 23*), the distribution of ASI sizes in our S1 and M1 samples was log-normal (Fig.2B), a feature thought to emerge from multiplicative dynamics(*22*). On the log scale the S group showed an overall shift to the left relative to the SW and EW groups, suggesting that the decrease in ASI during sleep obeyed a scaling relationship (Fig.2B, inset; 2C). Formal testing (see Methods) confirmed scaling when sleep was compared to either spontaneous wake (average scaling -20.1%, p = 0.784) or enforced wake (average

4

scaling -19.1%, p= 0.648). Monte Carlo simulations on bootstrapped data (see Methods) suggested that the change in ASI sizes between wake and sleep is not consistent with uniform scaling across all synapses, but rather with selective scaling, where a fraction of all synapses scales and the remaining portion does not. Of the models tested, the best fit was provided when the likelihood of scaling decreased quadratically with increasing ASI size (Fig.2D). This model fitted the actual data best assuming that a majority of all synapses (>80%) would scale and a minority (<20%) would be less likely to do so (Fig.2D).

Do morphological features of synapses predict the likelihood of scaling? Given the results in Fig. 2D, we asked whether distinguishing between small-medium synapses (bottom 80%) vs. large synapses would predict scaling vs. not-scaling. This distinction based on size was significant (p = 0.009; small ASI; S vs. SW -11.9%, p = 0.0002; S vs. EW -12.5%, p = 0.0001; large ASI; S vs. SW +0.7%, p = 0.999; S vs. EW +2.0% p = 0.994) (Fig.3A) and robust for scaling fractions around 80% (see Methods). In summary, these results indicate that the ASIs of most synapses decrease during sleep in a manner proportional to their size, and that the largest 20% of spines are less likely to scale.

Plastic changes may preferentially occur in spines that contain recycling endosomes(*24*), whose presence reflects increased turnover of membranes, glutamate receptors and other proteins that are essential to support activity-dependent structural changes(*13, 24, 25*). Indeed, only spines containing vesicles, tubules and multivesicular bodies (MVBs), most of which are considered of endosomal origin (*20*), showed significant scaling (p = 0.00003; vesicles/tubules +; S vs. SW -25.0%, p = 0.00001; S vs. EW -20.9%, p = 0.0008; vesicles/tubules -; S vs. SW -2.9%, p = 0.985; S vs. EW -2.8% p = 0.989)(Fig.3B,C).

A spine's structural plasticity may be constrained by the overall spine density of its dendritic branch(*26*). Although synaptic density by itself was unaffected by wake and sleep (p = 0.761), it interacted with the effect of sleep on ASI (p = 0.038): the ASI decrease with sleep was largest in less spiny dendrites (S vs. SW = -36.4%; S vs. EW = -25.3%) and smallest in dendrites with higher synaptic density (S vs. SW = 7.8%; S vs. EW = -8.2%) (Fig.3D).

By contrast, ASI decreased with sleep both in the spines with a spine apparatus(*27*) - a specialization of SER involved in calcium regulation and synthesis of transmembrane proteins - and in those without it(*28*) (Fig.3E). While spines facing an axonal bouton with one or more mitochondria were larger than spines lacking an axonal mitochondrion, scaling again occurred in both groups of spines (Fig.3F). In summary, ASI size scales down between wake and sleep in small and medium sized synapses (~80% of the total population), but is less likely to do so in synapses that are large (~20%) or in spines that contain no endosomes, and it is less marked in highly spiny dendrites.

Because HV is also strongly correlated with synaptic strength, we investigated changes in HV as a function of wake and sleep using a linear model that included the same random and fixed effects as for ASI (see Methods, LME Model for HV). Results were consistent with those with ASI (χ^2 = 6.942, df = 2, p = 0.031), with one additional interaction (condition x dendrite diameter): HV decreased most in the largest dendrites (S vs. SW = -31.8%; S vs. EW = -38.4%) and least in the smallest dendrites (S vs. SW = -4.7%; S vs. EW = 1.3%)(Fig.S3A,B). Like ASIs, HVs followed a log-normal distribution (Fig.S3C) and as a group, only the spines with vesicles, tubules and MVBs showed a significant downscaling in HV after sleep at an average value of dendrite diameter (vesicles/tubules +: S vs. SW = -20.8%, p = 0.0006; S vs. EW = -14.3%, p = 0.045; vesicles/tubules -: S vs. SW = 6.4%, p = 0.776; S vs. EW = 1.3%, p = 0.999) (Fig.S3D,E).

The ultrastructural demonstration of up- and downscaling of synapse sizes with wake and sleep supports the hypothesis that wake leads to a net increase in synaptic strength, whereas a core function of sleep is to renormalize synaptic strength through a net decrease(*16*). Ultrastructural analysis provides the morphological ground truth, but it is necessarily limited to small brain samples. However, synaptic scaling across the wake/sleep cycle is likely to be a general phenomenon, irrespective of species, brain region, and specific plasticity mechanisms(*16*). Here we found similar changes in two different cortical regions. Moreover, protein levels of GluA1-containing AMPA receptors are higher after wake than after sleep(*29*) across the entire cerebral cortex. Also, the number of immuno-labeled synaptic puncta increases with enriched wake and decreases with sleep in widespread regions of the fly brain(*30*). Finally, electrophysiological markers of synaptic efficacy also increase broadly after wake and decrease after sleep(*16*).

The scaling of synaptic size is not uniform, consistent with the requirement that learning during wake must potentiate synapses selectively, and with the hypothesis that selective renormalization during sleep favors memory consolidation, integration, and 'smart' forgetting(*16*). We do not know how scaling is apportioned between wake and sleep. During wake there may be a selective upscaling of a smaller proportion of synapses, because learning is limited to a particular environment(*31*); whereas downscaling during sleep may be broader, because the brain can sample its memories comprehensively and fairly when it is offline(*16*). We also cannot rule out that a few synapses may upscale in sleep(*16, 17*). Future studies labeling individual plastic events in the same synapses over wake and sleep may shed light on this issue. It will also be important to assess which molecular mechanisms are involved in the selective scaling of excitatory synapses in wake and sleep, and to evaluate possible changes in inhibitory synapses(*32*).

Finally, we found that the synapses that most likely escape scaling are those that are large, those that lack endosomes, as well as those in crowded dendritic branches. These features may represent

structural markers (besides molecular markers(*33*)) of synapses and associated memory circuits that are either committed or relatively stable despite the profound daily remodeling. We do not know, however, to what extent and over which time scale synapses may switch between this smaller pool of stronger, more stable synapses and the larger pool of weaker, more plastic synapses. An intriguing question is whether the subset of strong and stable synapses may originate preferentially from neurons at the top of the log-normal distribution of firing rates(*34*), whose level of activity seems to remain stable when the environment changes(*35*), or perhaps from neurons located in a specific layer (2/3 or 5).

Fig. 1 | Experimental groups and SBEM segmentation of cortical synapses. A, the 3 experimental groups: SW, spontaneous wake at night; EW, wake during the day enforced by exposure to novel objects; S, sleep during the day. Arrowheads indicate time of brain collection. **B**, percent of wake in each mouse (4 mice/group) during the last 6 hours before brain collection. **C**, schematic representation of mouse primary motor (M1, left) and somatosensory (S1, right) cortex with the region of SBEM data collection indicated in layer 2 (blue box). Reconstruction of 4 spiny dendritic segments in S1. **D**, some of the dendritic segments from SW, EW and S mice reconstructed in this study (all segments are shown in Fig.S1). Scale bar = 15 µm. **E,F,** raw image of a cortical spine containing a synapse and its 3D reconstruction (spine head in yellow, ASI in red; axonal bouton in green). Scale bar = 350 nm.
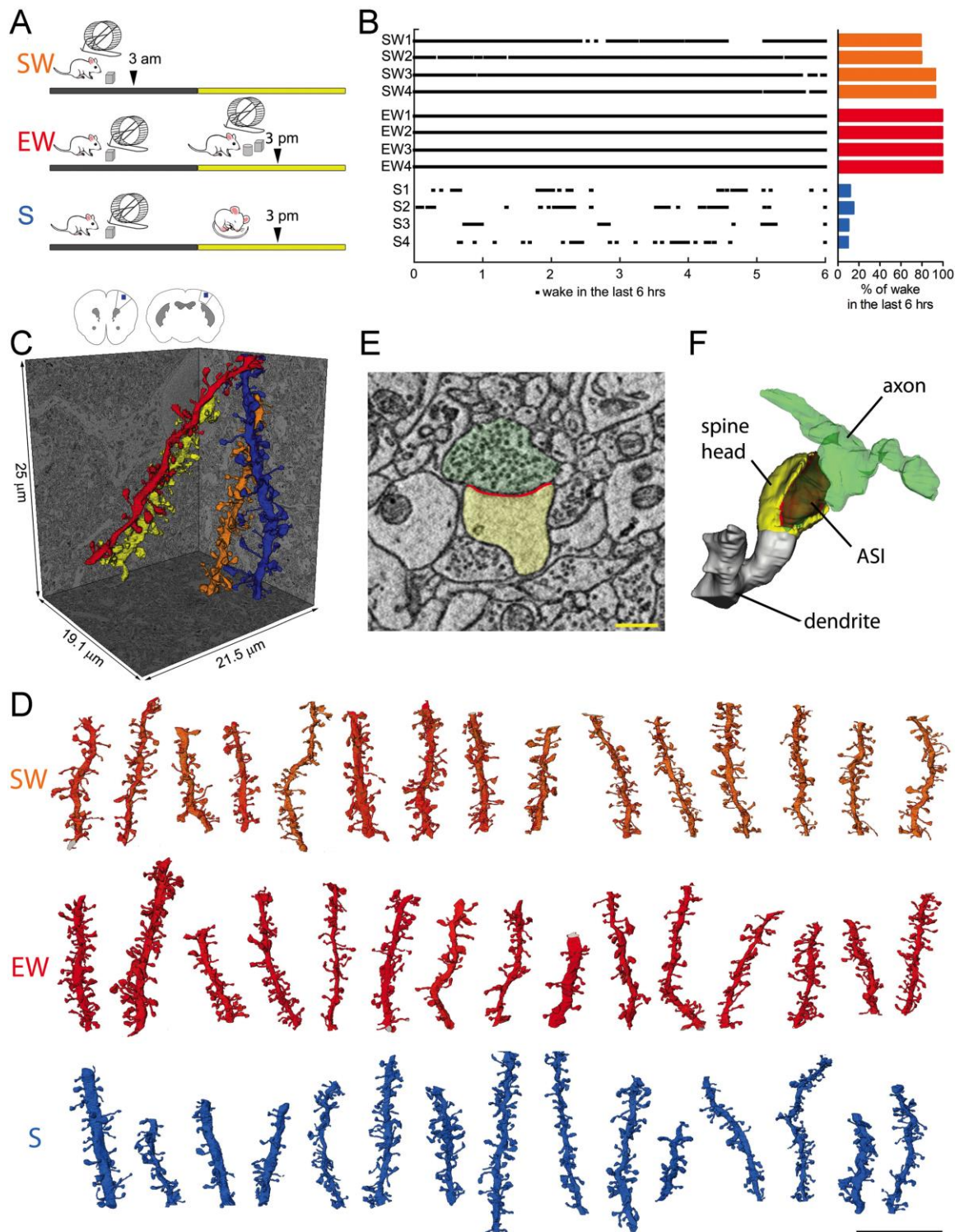
Fig. 2 | ASI size declines in sleep according to a scaling relationship. A, left, visualization of ASIs in one dendrite. Scale bar = 2.5 μm. Right, effect of condition: ASI size decreases in sleep (blue) relative to both spontaneous wake (orange) and enforced wake (red). ASI size is shown for all synapses, each represented by one dot. **, p< 0.01. **B,** log-normal distribution of ASI sizes in the 3 experimental groups. Inset, same on a log scale. **C**, the decrease in ASI size during sleep is due to scaling. **D**, Monte Carlo simulations comparing different models of scaling: size-dependent selective scaling (green) fits the actual data better than uniform scaling (asterisk) or selective scaling independent of size (brown; see also Methods).
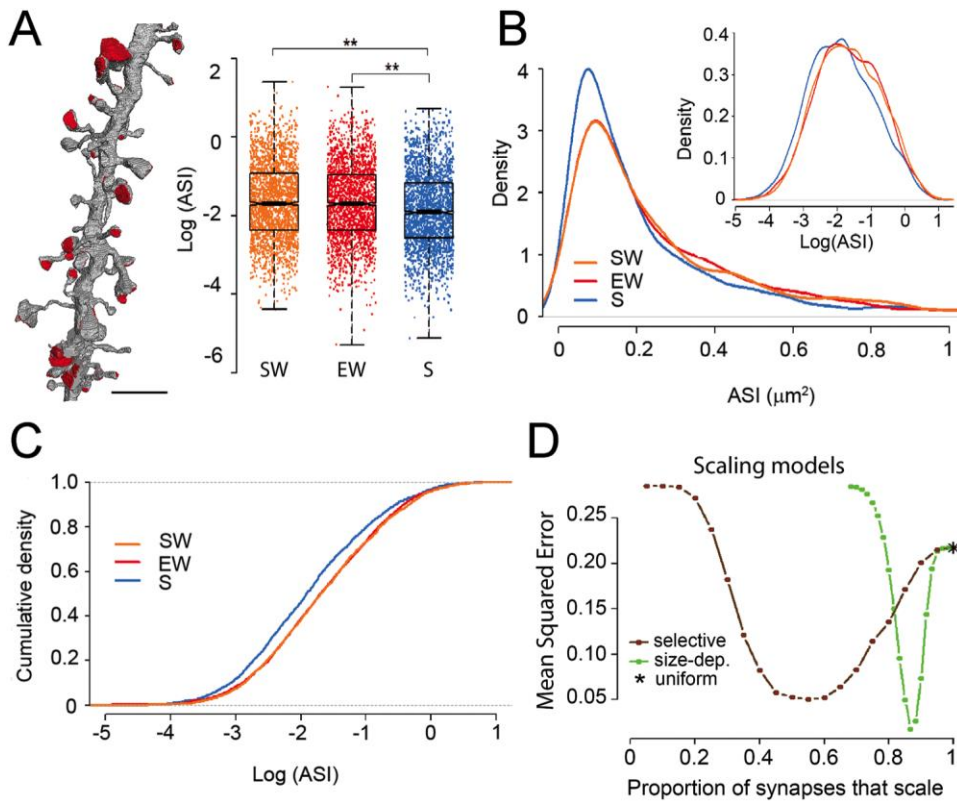
Fig. 3 | Scaling of ASI size is selective. A, the effect of sleep is present in small-medium synapses (80% of all synapses) but not in the largest ones (20% of all synapses); **B**, the effect of sleep is present in spines with non-SER elements (vesicles, tubules and multivesicular bodies, labeled "vesicles/tubules"); top image shows a multivesicular body (arrowhead) and a coated vesicle (asterisk); bottom image shows a non-SER tubule (arrowhead). **C**, the ASI decrease during sleep in spines with vesicles/tubules is due to scaling. **D,** the decline of ASI size in sleep is greatest in the dendrites with the lowest synaptic density (range: 0.17-1.24/μm^2); at the average value of synaptic density (vertical line; 0.70/μm^2), the mean overall decrease is -17.3% (S vs. SW -17.4%, p = 0.002; S vs. EW -17.3%, p = 0.002). **E,F,** ASI size declines in sleep independent of the presence of spine apparatus (asterisk) or mitochondria in the axonal bouton (arrowheads). Scale bars = 500 nm. Note that in all experimental groups, spines containing a spine apparatus or facing an axonal bouton with mitochondria are larger than spines lacking these elements. ** p< 0.01; *** p< 0.001.
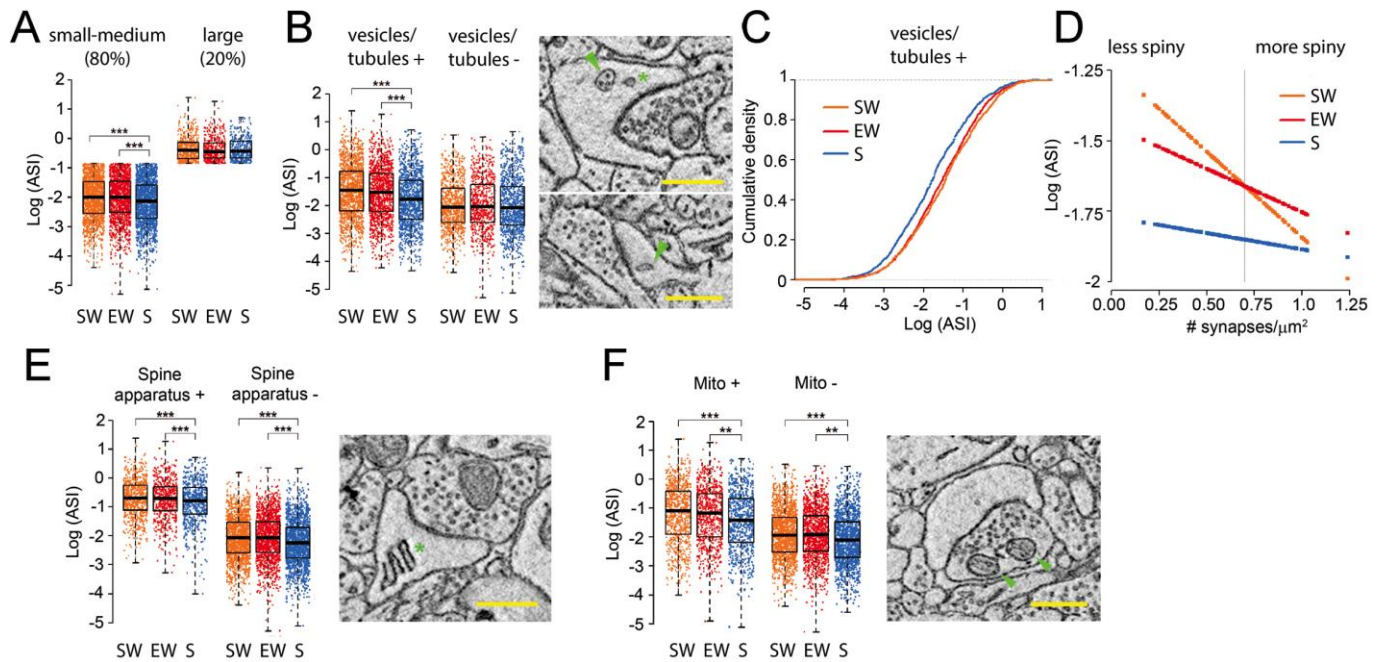
REFERENCES AND NOTES

1. S. Herculano-Houzel, The human brain in numbers: a linearly scaled-up primate brain. *Front Hum Neurosci* **3**, 31 (2009).
2. Y. Tang, J. R. Nyengaard, D. M. De Groot, H. J. Gundersen, Total regional and global number of synapses in the human brain neocortex. *Synapse* **41**, 258-273 (2001).
3. A. Holtmaat, K. Svoboda, Experience-dependent structural synaptic plasticity in the mammalian brain. *Nat Rev Neurosci* **10**, 647-658 (2009).
4. J. Nishiyama, R. Yasuda, Biochemical Computation for Spine Structural Plasticity. *Neuron* **87**, 63-75 (2015).
5. K. M. Harris, J. K. Stevens, Dendritic spines of CA 1 pyramidal cells in the rat hippocampus: serial electron microscopy with reference to their biophysical characteristics. *The Journal of neuroscience : the official journal of the Society for Neuroscience* **9**, 2982-2997 (1989).
6. N. L. Desmond, W. B. Levy, Synaptic interface surface area increases with long-term potentiation in the hippocampal dentate gyrus. *Brain research* **453**, 308-314 (1988).
7. P. A. Buchs, D. Muller, Induction of long-term potentiation is associated with major ultrastructural changes of activated synapses. *Proceedings of the National Academy of Sciences of the United States of America* **93**, 8040-8045 (1996).
8. C. E. Cheetham, S. J. Barnes, G. Albieri, G. W. Knott, G. T. Finnerty, Pansynaptic enlargement at adult cortical connections strengthened by experience. *Cerebral cortex* **24**, 521-531 (2014).
9. Y. Katz *et al.*, Synapse distribution suggests a two-stage model of dendritic integration in CA1 pyramidal neurons. *Neuron* **63**, 171-177 (2009).
10. M. Matsuzaki *et al.*, Dendritic spine geometry is critical for AMPA receptor expression in hippocampal CA1 pyramidal neurons. *Nature neuroscience* **4**, 1086-1092 (2001).
11. M. Bosch *et al.*, Structural and molecular remodeling of dendritic spine substructures during long-term potentiation. *Neuron* **82**, 444-459 (2014).
12. D. E. Feldman, Synaptic mechanisms for plasticity in neocortex. *Annu Rev Neurosci* **32**, 33-55 (2009).
13. R. L. Huganir, R. A. Nicoll, AMPARs and synaptic plasticity: the last 25 years. *Neuron* **80**, 704-717 (2013).
14. C. von der Malsburg, Self-organization of orientation sensitive cells in the striate cortex. *Kybernetik* **14**, 85-100 (1973).
15. M. Chistiakova, N. M. Bannon, J. Y. Chen, M. Bazhenov, M. Volgushev, Homeostatic role of heterosynaptic plasticity: models and experiments. *Front Comput Neurosci* **9**, 89 (2015).
16. G. Tononi, C. Cirelli, Sleep and the price of plasticity: from synaptic and cellular homeostasis to memory consolidation and integration. *Neuron* **81**, 12-34 (2014).
17. B. Rasch, J. Born, About sleep's role in memory. *Physiol Rev* **93**, 681-766 (2013).
18. W. C. Abraham, A. Robins, Memory retention--the synaptic stability versus plasticity dilemma. *Trends Neurosci* **28**, 73-78 (2005).
19. W. Denk, H. Horstmann, Serial block-face scanning electron microscopy to reconstruct three-dimensional tissue nanostructure. *PLoS Biol* **2**, e329 (2004).
20. J. R. Cooney, J. L. Hurlburt, D. K. Selig, K. M. Harris, J. C. Fiala, Endosomal compartments serve multiple hippocampal dendritic spines from a widespread rather than a local store of recycling membrane. *The Journal of neuroscience : the official journal of the Society for Neuroscience* **22**, 2215-2224 (2002).
21. P. S. Holcomb *et al.*, Synaptic inputs compete during rapid formation of the calyx of Held: a new model system for neural development. *The Journal of neuroscience : the official journal of the Society for Neuroscience* **33**, 12954-12969 (2013).
22. Y. Loewenstein, A. Kuras, S. Rumpel, Multiplicative dynamics underlie the emergence of the log-normal distribution of spine sizes in the neocortex in vivo. *The Journal of neuroscience : the official journal of the Society for Neuroscience* **31**, 9481-9488 (2011).
23. M. Cane, B. Maco, G. Knott, A. Holtmaat, The relationship between PSD-95 clustering and spine stability in vivo. *The Journal of neuroscience : the official journal of the Society for Neuroscience* **34**, 2075-2086 (2014).
24. M. Park *et al.*, Plasticity-induced growth of dendritic spines by exocytic trafficking from recycling endosomes. *Neuron* **52**, 817-830 (2006).

25. J. H. Tao-Cheng *et al.*, Trafficking of AMPA receptors at plasma membranes of hippocampal neurons. *The Journal of neuroscience : the official journal of the Society for Neuroscience* **31**, 4834-4843 (2011).

26. A. J. Holtmaat *et al.*, Transient and persistent dendritic spines in the neocortex in vivo. *Neuron* **45**, 279-291. (2005).

27. N. Holbro, A. Grunditz, T. G. Oertner, Differential distribution of endoplasmic reticulum controls metabotropic signaling and plasticity at hippocampal synapses. *Proceedings of the National Academy of Sciences of the United States of America* **106**, 15055-15060 (2009).

28. L. E. Ostroff, C. K. Cain, J. Bedont, M. H. Monfils, J. E. Ledoux, Fear and safety learning differentially affect synapse size and dendritic translation in the lateral amygdala. *Proceedings of the National Academy of Sciences of the United States of America* **107**, 9418-9423 (2010).

29. V. Vyazovskiy, C. Cirelli, M. Pfister-Genskow, U. Faraguna, G. Tononi, Molecular and electrophysiological evidence for net synaptic potentiation in wake and depression in sleep. *Nature neuroscience* **11**, 200-208 (2008).

30. D. Bushey, G. Tononi, C. Cirelli, Sleep and synaptic homeostasis: structural evidence in Drosophila. *Science* **332**, 1576-1581 (2011).

31. H. Makino, R. Malinow, Compartmentalized versus global synaptic plasticity on dendrites controlled by experience. *Neuron* **72**, 1001-1011 (2011).

32. G. W. Knott, C. Quairiaux, C. Genoud, E. Welker, Formation of dendritic spines with GABAergic synapses induced by whisker stimulation in adult mice. *Neuron* **34**, 265-273 (2002).

33. G. H. Diering, A. S. Gustina, R. L. Huganir, PKA-GluA1 coupling via AKAP5 controls AMPA receptor phosphorylation and cell-surface targeting during bidirectional homeostatic plasticity. *Neuron* **84**, 790-805 (2014).

34. G. Buzsaki, K. Mizuseki, The log-dynamic brain: how skewed distributions affect network operations. *Nat Rev Neurosci* **15**, 264-278 (2014).

35. Y. Ziv *et al.*, Long-term dynamics of CA1 hippocampal place codes. *Nature neuroscience* **16**, 264-266 (2013).

ACKNOWLEDGEMENTS

SUPPLEMENTARY MATERIALS

www.sciencemag.org/content/vvvv

Materials and Methods

Figs. S1-S3

Tables S1, S2

References (36-53)